2528-9705

Örgütsel Davranış Araştırmaları Dergisi
Journal Of Organizational Behavior Research
Cilt / Vol.: 3, Sayı / Is.: S2, Yıl/Year: 2018, Kod/ID: 81S2434

NUMERICAL STUDY OF ENERGY STORAGE EFFICIENCY IMPROVEMENT IN RESIDENTIAL BUILDINGS BY ADDING NANOPARTICLES IN PHASE CHANGE MATERIAL

Mehdi AMINI, Mohammad Hassan NOBAKHTI*, Morteza KHAYAT

Faculty of Mechanics, Electrical Power and Computer, Science and Research Branch, Islamic Azad University, Tehran, Iran.

***Corresponding Author:**
Email: m.nobakhti@srbiau.ac.ir

ABSTRACT

Today, the increasing consumption of fossil fuels and their harmful effects on the environment, as well as increasing energy consumption in heating and cooling of the buildings, has led to the use of energy storage systems with phase change materials. In the present study, the amount of thermal energy storage in the building wall has been investigated by using the addition of two types of copper (Cu) and aluminum oxide (Al2O3) nanoparticles in octadecane phase change material. To optimizing the thermal energy storage by phase change material, the parameters such as nanoparticle type, nanoparticle concentration, displacement of the position of the octadecane layer, and also the optimal thickness of the phasechange material layer are investigated. Addition of Cu nanoparticles in all volumetric percentages (0.5%, 1%, 3%, 5%) compared to Al2O3 with the same volumetric percentages (1% and 3%), and the pure octadecane, shows a higher increase in thermal energy storage. In the presence of Cu nanoparticles, the greatest increase in thermal energy storage is observed in 1% vol. The optimum thickness is 1.2 centimeters in the case where the phase change material is located behind the inner wall layer, which is 1.5 centimeters when the phasechange material is between the brick and the gypsum and soil layer (near layer to the external wall) which reduces the weight of the octadecane by 30%.

Keywords: *Phase Change Material, Octadecane, Cu nanoparticles, Al2O3 nanoparticles, Buliding wall*

INTRODUCTION

Increasing energy consumption in heating and cooling has attracted global attention to the use of renewable energy, as today use of solar energy plays a significant role in reducing fossil fuels. One of the main problems with solar energy is inconsistency at the peak of energy consumption with the energy production process. The development of energy storage systems is intended to eliminate the mismatch between storage and consumption. The storage of latent heat that is based on the absorption (release) of energy during phase change from solid to liquid, liquid to gas and vice versa, due to providing high amount of energy and energy storage at constant temperature, has been considered in recent decades. The purpose of energy storage is to find a way to reduce the electrical energy consumption of the system and reduce costs. Years after the use of phase change materials and with the development of nanoscale technology, in order to change the properties of heat transfer and increase the thermal conductivity and as a result, a significant increase in the rate of heat transfer in these materials, particles in the nanometeric scale (usually metal or metal oxides) added to them. With the development of nanoparticle research, these particles do not only affect the thermal

Geliş tarihi/Recieved: 03.04.2018 – Kabul tarihi/Accepted: 09.04.2018 – Yayın tarihi/Published: 21.08.2018

conductivity of the material, but also affect other physical properties, such as fluid heat capacity. So far, many studies have been done on phase change materials with nanoparticles.

Liu et al. (2015) reviewed the history of properties and conditions of the first type of nano phase change materials called NEPMC. This type of nano phase change material is produced in the form that filled with a phase change material in the inner core. While the phase change material surrounded by a membrane. In their research, the heat transfer properties of nano phase change material have been investigated. Raja et al. (2018) examined the effect of adding copper oxide nanoparticles (CuO) to paraffinic phase change material on thermal conductivity. The results show that the addition of 2% of nanoparticles mass to phase change material by ultrasonic waves, increases the amount of thermal conductivity by 76%. Parameshwaran et al. (2013) examined the effect of adding spherical silver nanoparticles to organic phase change materials at different mass concentrations. The results show that the silver nanoparticles do not chemical reaction with the phase change material, and hence the nano phase change materials is chemically stable. Park et al. (2014) explored the effect of adding iron oxide nanoparticles (Fe3O4) to paraffinic phase change materials. The results showed that the addition of iron oxide particles to the phase change material increased the thermal conductivity of the material from 23 $\frac{w}{m.k}$ to 33 $\frac{w}{m.k}$.

Motahar et al. (2017) investigated the freezing process of a phase change material containing TiO2 nanoparticles for energy storage. The phase change material used in their work is n-octadecane. The experiment was carried out in a rectangular chamber that cooling process is done from a vertical wall. Stefan number in this study ranges from 0.17 to 0.239. Benli and Durmuş (2009) used a laboratory for the heating of the Na2SO4.10H2O phase change material with additives that prevent fuzzy decomposition and energy loss. They found that 40 to 60 percent of the PCM latent heat potential could be released, while nearly half of the ability of the PCM substance was not used. They also tested polyethylene glycol and CaCl2.6H2O as a PCM material for greenhouse heating of 7.2 m^2 and compared traditional greenhouses with greenhouses with a PCM storage system and found that the energy efficiency of greenhouses combined with solar collectors is approximately 59%, and this system is capable of maintaining an indoor greenhouse temperature of 8°C throughout the night, with an environmental temperature up to -0.6 °C.

Melting of PCM in a rectangular chamber is investigated in a laboratory experiment by Stritih (2004) the results of the experiment are compared with the analytical data based on the conduction heat transfer mechanism. The results showed that only at the beginning of the melting process, analytical data had good agreement with experimental results. But after a melting time, the results have been significantly different. Elgafy and Lafdi (2005) made a special composite by adding nano-carbon fibers with an average diameter of 100 mm and an average length of 20 mm in paraffin. Their studies focused on the heat transfer parameters during the freezing process. They found that the thermal conductivity of the composite increased in particular by increasing the mass fraction of nano-fiber in the composite. Even with 1% of nanoparticulate fiber, a decrease of 23% was observed during freezing. They also found that adding fiber to PCM does not reduce storage capacity. As a result, the output power is linearly increased by increasing the mass fraction of carbon fiber. Their results showed that with a uniform distribution of fibers in PCM, a greater increase in the performance is obtained.

Nayak et al. (2006) examined the effect of using the blade on the phase change material side in order to increase the heat transfer with in this material. For this purpose, three different geometric structures have been used. The results show that the use of rod blades has more efficiency and a uniform temperature distribution. Sanusi (2010) studied the use of nanoparticles in paraffin to increase heat transfer in the phase change material. The results show that the use of nanoparticles in paraffin can have a longer and better temperature control than pure paraffin.

Leland and Recktenwald (2003) numerically optimized the geometry of a PCM heat sink used for severe environmental conditions by ignoring the effect of the convection in the melted PCM, the effects of the edge on the boundary of the environment and the heat dispersion effects in the heat sink. Zheng and Wirtz (2000, 2001 and 2004) used numerical and experimental models to optimize the performance of heat sinks. The phase change material used was $C_5H_{12}O_3$ with a melting point of 83°C. Gopalan et al. (2016) numerically evaluated the thermal performance of a PCM heat sink using porous media as a heat conduction enhancer. The results showed that the heat sink with the porous medium had a better performance than the heat sink with PCM alone. Pakrouh et al. (2015) carried out a numerical evaluation of the geometric optimization of PCM heat sink with blades, and their results showed that a complex relationship between PCM percentages and TCE volumes and optimal PCM percentages were found.

With the development of phase change materials, the use of these materials in walls, roofs, floors and shutters has expanded as part of the heating-cooling system of buildings. The use of PCMs in buildings pursues two goals, which include using the natural warmth of the sun to heat or use the cold of the night to cool. The use of these materials in the walls, in addition to their lighter ones, also provides energy storage.

In this research, the issue of energy storage in residential building walls with phase change materials has been investigated. Phase change materials are used in a wide range of temperatures and in the subject of the building, these materials must have a melting temperature in the proper range for ventilation of the building. For this reason, the octadecane phase change material is selected. The melting temperature of this material is about 28°C. In order to verify the thermal performance, the walls of the building consisting of stone, mortar, brick, plaster, soil and octadecane phase change material have been considered, and the modeling has been carried out for a warm summer day for the Tehran region. Then, due to the low thermal conductivity coefficient of the octadecane, to improve the heat transfer process, aluminum oxide nanoparticles with volumetric percentage of 1% and 3% and copper with volumetric percentages of 0.5%, 1%, 3% and 5% have been used in the base of the octadecane and three different walls without PCM and PCM with two types of nanoparticles are investigated.

The main goal is to reduce energy consumption in the building and to find the optimal mode of phase change material function, which is achieved by numerical simulation of the above problem in fluent software.

The process of numerical simulation and assumptions used is that at first the fluid is completely stationary at a constant temperature between the temperature of the cold and hot walls. Then, with the onset of the phase change process, the viscous and incompressible flow, conduction and free convection heat transfer starting with the assumption of the Boussinesq approximation in the problem environment. After numerical modeling and analysis, the effect of parameters such as nanoparticle concentration, type of nanoparticles as well as wall geometry have been investigated.

PROBLEM GEOMETRY AND NUMERICAL SIMULATION

Geometry and grid generation

Problem geometry is a wall which the phase change material is embedded inside it. The dimensions of the wall are considered in accordance with Table. 1, and the layers of the wall from the inner layer side, are the plaster, the phase change material, the plaster-soil, the brick, the mortar and the stone. The Ansys mesh software is used to generating grid and geometry. In Figure. 1, an outline of the problem geometry is shown.

Table 1: Dimensions of the layers of the wall

Materials of wall layer	(mm) Dimension
Stone	20
Mortar	40
Brick	200
Soil and Plaster	30
PCM	20
Plaster	10
Wall length	4000
Wall High	2800

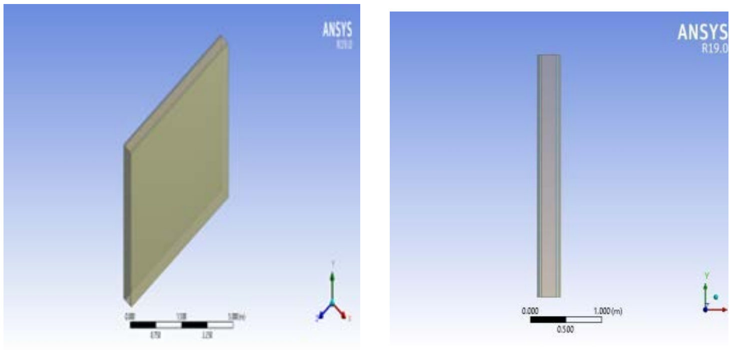

Figure 1: The geometry of the wall

Grid quality greatly affects the solution convergence process. Finding an optimal grid that answers are independent of that grid is quite experimental and time-consuming. Typically, to find such a grid, the numerical simulation output parameters are mapped according to the number of grid nodes, so that ultimately, with increasing number of nodes, no change in the parameters is obtained. Figure. 2, shows the final grid of the problem geometry. The type of this grid is structure.

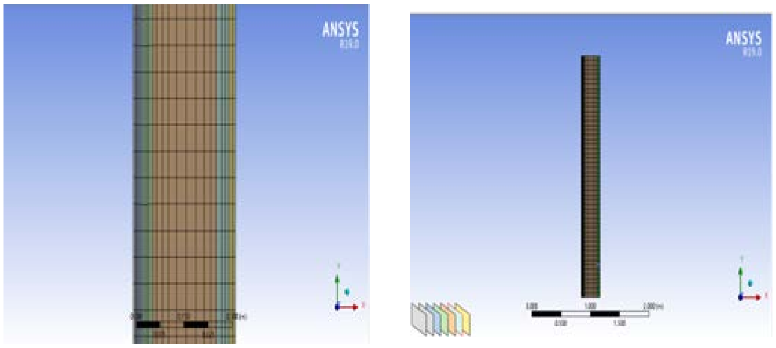

Figure 2: Generated grid

Governing equations and solving method

In this study, the enthalpy-porosity technique is used, instead of tracing the common solid-liquid boundary explicitly. The liquid-solid paste region behaves as a porous portion of the fluid fraction, and the components of proper momentum sources are added to the momentum equations for the loss of pressure due to the presence of solids. When using the freezing/melting model in relation to the modeling of the reaction components transfer, there is no mechanism for limiting the reaction in the liquid region, that is, the reactions are solved everywhere. In the enthalpy-porosity technique, the fusion boundary is not explicitly detected. Instead, a value called the volume fraction of the liquid, which represents the fraction of the volume of the cell that is in the form of a liquid, is associated with each cell in the domain of the solution. The liquid fraction is calculated in each repetition based on the enthalpy balance. The paste region is a region in which the liquid fraction is between 0 and 1. The paste region is modeled as a pseudo-porous medium in which porosity decreases from 1 to 0. When a substance becomes solid in a cell, the porosity becomes zero and hence the speed reaches zero.

Relations (1) and (2), show the continuity and momentum equations.

$$\partial_t(\rho) + \partial_i(\rho u_i) = 0 \qquad (1)$$

$$\partial_t(\rho u_i) + \partial_i(\rho u_i u_j) = -\partial_i(P) + \rho g_i + \mu \partial_{jj}(u_i) + S_i \qquad (2)$$

The component of momentum source resulting from the reduction of porosity in the paste region is obtained from equation (3).

$$S_i = C(1-\beta)^2 \frac{u_i}{\beta^3 + \varepsilon} \qquad (3)$$

Where C is a constant for the paste region between 10^4 and 10^7 (Al-Abidi et al., 2013) Also, ε is a small number of 0.001 to avoid dividing by zero.

The enthalpy is calculated in terms of the sum of the sensible enthalpy h and the latent heat ΔH from relations (4) and (5).

$$H = h + \Delta H \qquad (4)$$

$$h = h_{ref} + \int_{T_{ref}}^{T} C_p dT \qquad (5)$$

The value of latent heat can vary between zero (for solids) and L (for liquid). Therefore, ΔH is obtained from relation (6).

$$\Delta H = \beta L \qquad (6)$$

For the melting and freezing problems, the energy equation is considered in the form of relation (7).

$$\partial_t(\rho h) + \partial_t(\rho \Delta H) + \partial_i(\rho u_i h) = +\partial_i(k \partial_i T) \qquad (7)$$

For natural convection, instead of the density definition, as a function of temperature, one can use the Boussinesq approximation according to equation (8) to achieve faster convergence. This model is accurate when the variation of density is small.

$$\rho = \rho_0(1 - \alpha \Delta T) \qquad (8)$$

Using this model, the density is considered constant for all solvable equations, except for the buoyancy term in the momentum equation which obtained from relation (9).

$$(\rho - \rho_0)g \cong -\rho_0 \alpha (T - T_0) g \qquad (9)$$

In this research, the Boussinesq approximation is used to calculate the time-dependent natural convection in closed environment.

To freezing and melting a pure material, the phase change occurs at a specific melting temperature T_{melt}. However, for a multi components mixture, there is a freezing/melting paste region between the low temperature of the solidification and the high temperature of liquidation. When a multi components liquid convert to solid, the soluble matter is dispersed from the solid phase to the liquid phase. This effect is determined by the dispersion coefficient of the soluble matter i, which is represented by K_i and is equal to the ratio of solid mass fraction to mass fraction of liquid at the interface.

In the numerical solution method, the solid and liquid temperatures in the multi components mixture are obtained from relationships (10) and (11).

$$T_{solidus} = T_{melt} + \sum_{solutes} \frac{m_i Y_i}{K_i} \qquad (10)$$

$$T_{liquidus} = T_{melt} + \sum_{solutes} m_i Y_i \qquad (11)$$

The liquidification gradient of the i-th component, which is m_i, is obtained from $T_{eutectic}$ temprature, the lowest melting point of the material in which the frozen crystals and the liquid phase are in equilibrium, and the mass fraction $Y_{i,eutectic}$, according to equation (12).

$$m_i = \frac{T_{eutectic} - T_{melt}}{Y_{i,eutectic}} \qquad (12)$$

The volume fraction of the liquid is obtained from equation (13).

$$\beta = \frac{T - T_{solidus}}{T_{liquidus} - T_{solidus}} \qquad (13)$$

This relationship is for temperature between $T_{liquidus}$ and $T_{solidus}$. If the temperature is less than $T_{solidus}$, then $\beta = 0$, and if the temperature is greater than $T_{liquidus}$, then $\beta = 1$. Although the nanofluid of this study contains very low amounts of solid nanoparticles, the same low amounts will affect the nanofluid properties. In this study, relations (14) and (15) for density and specific heat capacity of nanofluid at reference temperature have been used (Jourabian et al., 2014)

$$\rho_{nf} = (1-\varphi)\rho_f + \varphi\rho_s \qquad (14)$$

$$(\rho C_p)_{nf} = (1-\varphi)(\rho C_p)_f + \varphi(\rho C_p)_s \qquad (15)$$

The base fluid density, which is the same phase change material, is variable with temprature and is obtained from equation (16).

$$\rho_f = \frac{860}{0.001(T - 298.15) + 1} \qquad (16)$$

The dynamical viscosity of the nanofluid is also calculated using relations (17) and (18) (Arıcı et al., 2017).

$$\mu_{npcm} = 0.983\mu_{pcm}\exp(12.959\varphi) \qquad (17)$$

$$\mu_{pcm} = 0.001\exp(-4.25 + \frac{1790}{T}) \qquad (18)$$

The thermal conductivity of the nanofluid at any given time, taking into account the changes in the thermal conductivity coefficient of the phase change material with temperature (to improve the accuracy of the calculations), is obtained from equation (19).

$$k_{npcm} = \frac{k_{np} + 2k_{pcm} - 2(k_{pcm} - k_{np})\varphi}{k_{np} + 2k_{pcm} + (k_{pcm} - k_{np})\varphi} k_{pcm} \qquad (19)$$

In this case, if the temperature is less than $T_{solidus}$, $k_{pcm} = k_s$ and if the temperature is greater than $T_{liquidus}$, $k_{pcm} = k_f$. Now, if the temperature is between $T_{solidus}$ and $T_{liquidus}$, k_{pcm} is obtained from equation (20) (Arıcı et al., 2017).

$$k_{pcm} = (1-\beta)k_s + \beta k_f \qquad (20)$$

k_f and k_s are the thermal conductivity coefficients of the phase change material, respectively, in liquid and solid state, which for octadecane are 0.148 $\frac{w}{m.k}$ and 0.358 $\frac{w}{m.k}$ respectively.

In the case of the addition of nanoparticles to phase change material, for the calculation of density, thermal conductivity and nanofluid viscosity at any time, and solving energy and momentum equations, the user defined function(UDF) is used in fluent software.

Assumptions and material properties

For modeling the problem, the following assumptions are considered:

- Properties of material in solid and liquid phases are constant.
- The nanofluid is modeled as a single phase fluid, and the effects of adding nanoparticles on the phase change material are applied.
- Phase change will occur at constant temperature.
- The boundary condition on one side of the wall is considered as a constant heat flux.
- The problem is considered steady.
- An incompressible fluid is considered.
- The heat flux is considered constant.

The ambient temperature of the outside of the building is considered for Tehran on the 29th of August, which is the warm days of the year, based on meteorological data at different times of the day. These temperature changes are shown in Figure 3. According to this figure, the average outside temperature is assumed to be 35°C. The heat flux equivalent to the radiation of the sun in Tehran city on the wall of the building, is equal to 950 $\frac{w}{m^2}$.

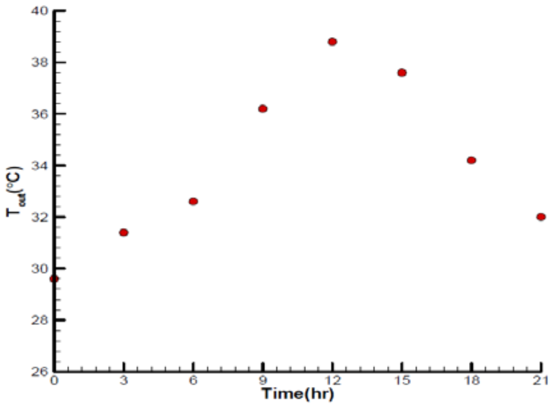

Figure 3: Exterior ambient temperature of the building for different hours in Tehran on the 29th of August

The thermo physical properties of the octadecane phase change material and the building materials of the wall along with the nanoparticles used in the present study are presented in Tables. 2 and 3, respectively.

Table 2: Thermophysical properties of phase change material

Phase Change Material	Octadecane
$(\frac{W}{m.K})$ Conduction heat coefficient	0.358
$(\frac{J}{kg.K})$ Specific heat capacity	1934
$(\frac{kg}{m^3})$ Density	865
(°C) Melting temperature	27
$(\frac{kJ}{kg})$ Heat of fusion	243.5

Table 3: Thermo physical properties of wall layers and nanoparticles

Type of material	Conduction heat coefficient ($\frac{W}{m.K}$)	Specific heat capacity ($\frac{J}{kg.K}$)	Density ($\frac{kg}{m^3}$)
Stone	2.8	775	2630
Mortar	1.4	780	1860
Brick	1.7	800	1700
Soil and Plaster	0.15	2000	1200
Plaster	0.16	840	950
Al2O3	36	765	3600
Cu	387	381	8978

Grid independency

To ensure that the solutions are independent of the grid (number of nodes), the volume fraction of the liquid (β), which is the most important parameter related to the impact of the use of phase change material, is provided for several computational grid which are shown in the Table. 4. This parameter is calculated for a period of 12 hours and is shown in Figure 4. It should be noted that in all cases, environmental conditions, model geometry and thermo physical properties are assumed constant. Regarding the results of Table. 4 and Figure. 4, the grid is used with the number of elements 129064.

Table 4: Compares the volume fraction of the liquid in 720 seconds for different grids

Number of elements	(β)
78336	0.6098
129064	0.6101
246519	0.6106

In order to evaluate the quality of the grid, skewness index is used, which means the proximity of the elements created in a balanced manner. The generated grid is acceptable, when the average value of this index is less than 0.95. If the average value of this index is between 0.95 and 1, the generated grid will be unacceptable. The value of this index for the optimal grid used in this study is 0.007, which indicates that the generated grid is very favorable. No matter how close this number is to zero, the better the grid quality.

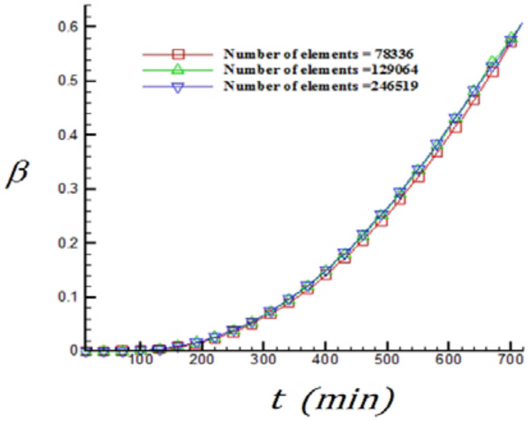

Figure 4: Comparing the volume fraction of the liquid in 720 seconds for different grids

RESULTS

Validation

In numerical simulations, the results of the work should first be compared with laboratory data or other numerical simulation to ensure the accuracy of the results. One of the most sensitive and important variables in the numerical simulation of the present study is the volume fraction of the liquid (β), since, after obtaining this parameter, it is determined how much of the phase change material is available in liquid form. Also, the volume fraction of a liquid at a time when its value reaches 1, indicates that the total phase change material has melted and if the heat flux continues, the temperature of the object is increased and the selected phase change material is not effective.

In order to validate the solving method, the geometry used by Darzi et al. (2013) has been used. First of all the grid generation of this geometry is carried out by Ansys mesh software. In the final stage, after applying the initial conditions and reference boundary conditions, the numerical simulation is done by using the governing equations of this research.

In reference (Darzi et al. 2013), the flow of air passing through the radiators, including the phase change material has been analyzed in a two-dimensional form. Figure. 5, shows the schematic geometry of the reference, which consists of a radiator in the corner of the room. During the day, the room's hot air enters the entrance, and after exchanging heat with PCM plates, it will transfer part of its heat to these plates and the radiator output will have a cooler air than the input. In Figure. 6, the dimensional characteristics of the plates containing PCM are depicted. In order to verify the results of this research, the dimensions of the first row indicated in Figure. 6, (Case1) have been used.

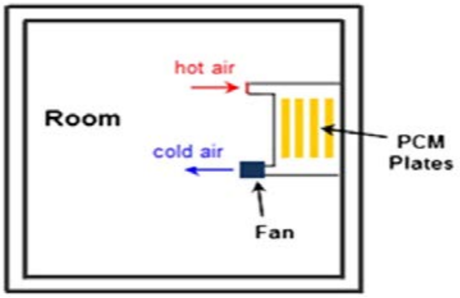

Figure 5: Reference geometry (Darzi et al., 2013)

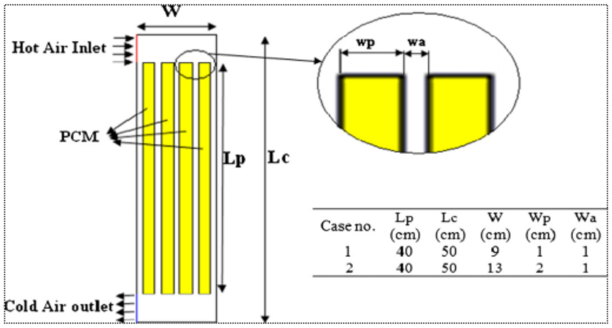

Case no.	Lp (cm)	Lc (cm)	W (cm)	Wp (cm)	Wa (cm)
1	40	50	9	1	1
2	40	50	13	2	1

Figure 6: Dimensions of plates containing phase change material of reference research (Darzi et al., 2013)

Table. 5, shows the thermo physical properties of the reference phase change material (Darzi et al., 2013), which is the SP22A17. The reason for choosing this material is the suitability of the melting temperature range as well as the low volumetric expansion coefficient during the melting process.

Table 5: Thermo physical properties of the phase change material SP22A17

Phase Change Material	SP22A17
$(\frac{W}{m.K})$Conduction heat coefficient	0.6
$(\frac{J}{kg.K})$ Specific heat capacity	2500
$(\frac{kg}{m^3})$ Density	1480
(°C) Melting temperature	22-24
$(\frac{kJ}{kg})$ Heat of fusion	150
$(\frac{1}{K})$ Expansion coefficient	0.001
$(\frac{mm^2}{s})$ Kinematical viscosity	111.1

In the reference paper, numerical analysis was performed in two modes of day and night, and for two different values of Stefan number, as well as two values of input mass and three air incoming air temperatures, but in order to verify the numerical solution method of the present study, only one value of Stefan number (Ste =0.1) was simulated at day mode and at an inlet air temperature of T= 29° C. The air flow and phase change material are assumed unsteady, incompressible and laminar and is modeled in two-dimensional form. The heat exchanger is assumed to be isolated, and the mass flow rate of the air is assumed to be constant equal to 0.018 $\frac{kg}{s}$. The room temperature is assumed to be constant. The grid generation of reference geometry is shown in Figure. 7, with a number of structure elements of 45000.

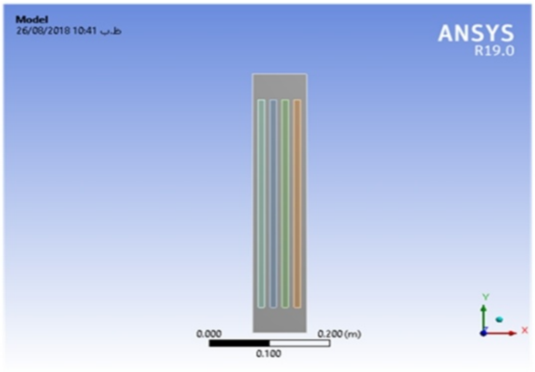

Figure 7: Modeling reference geometry

The turbulence model Standard K-epsilon is used to model the turbulence of the air flow inside this heat exchanger. Solidification/Melting model is also used to model PCM material. To validation the present study, Figure. 8, which represents the volume fraction of liquid of phase change material, is used. In this figure, three graphs are presented for the state (a), which is related to the geometry of the day. Each of these graphs is plotted by the number of Stefan and the amount of inlet mass flow rate associated with the air inlet. But as stated, in the present study, only for one Stefan number (Ste =0.1) in day mode and at an inlet air temperature (T= 29° C) numerical simulation is done. Given the fact that the analysis of PCM materials is very time-consuming and involves very high computational costs, a phase change diagram has been obtained to check the validity of the work up to 178 minutes since the start of the analysis.

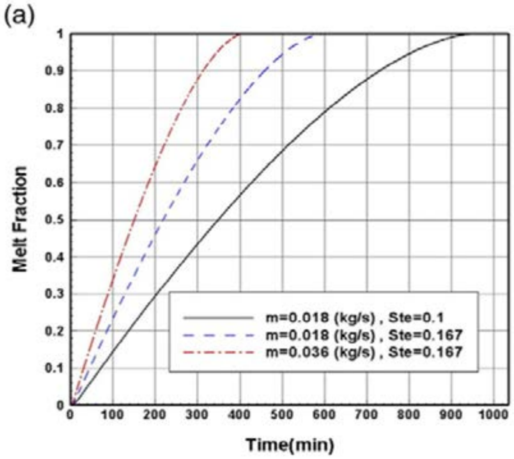

Figure 8: Volume fraction of liquid of phase change material versus time of reference research (Darzi et al., 2013)

After grid generation, the governing equations are solved by numerical methods by using the assumptions of the reference article. Comparison of the numerical results of this study with reference (Darzi et al. 2013), is shown in Figure. 9. The average relative error is 2.9 %, which indicates a very good agreement.

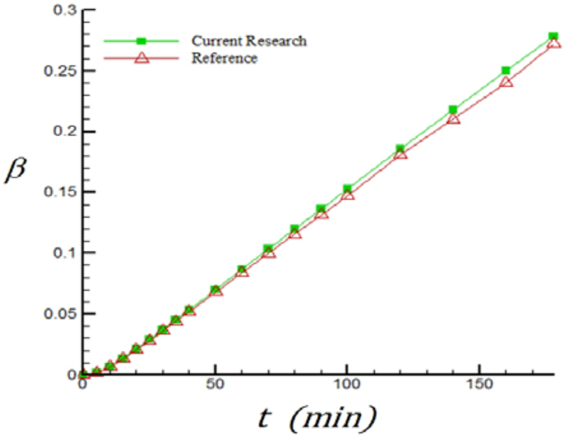

Figure 9: Comparing the results of reference research (Darzi et al., 2013) with present study

In Figure. 10, the temperature contours derived from the numerical solution method of the present study are compared with the reference article, qualitatively for 120 minutes, which are highly adapted.

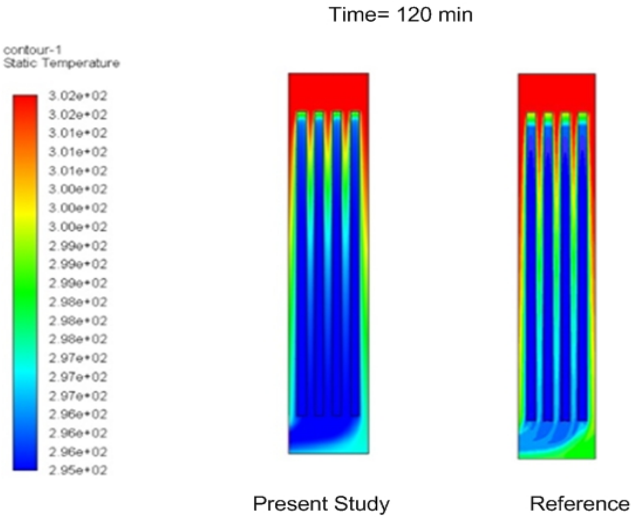

Figure 10: Qualitative comparison of temperature contours in 120 minutes

The Effect of phase change material on System Performance

Figure. 11, shows the liquid volume fraction (β) of the octadecane phase change material over time in a 12-hour interval. The liquid fraction is initially zero and then reaches 0.55 at the end of the time, indicating that more than half of the phase change material has been melted. The reason of the liquid fraction equal to zero at the initial time, is due to the initial temperature of 25°C (lower than the PCM melting temperature), which by increasing the temperature, when this temperature reaches the melting point of the phase change material, the liquid fraction begins to change.

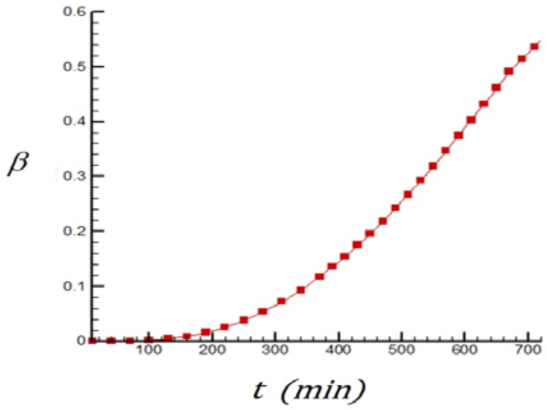

Figure 11: Changes in volume fraction of liquid relative to time

Figure. 12, shows the average interior wall surface temperature change for two modes without phase change material along with phase change material. It can be seen that when the phase change material is used, the interior surface temperature changes are negligible, due to the fact that the phase change material does not completely melt and absorbs a large part of the thermal energy.

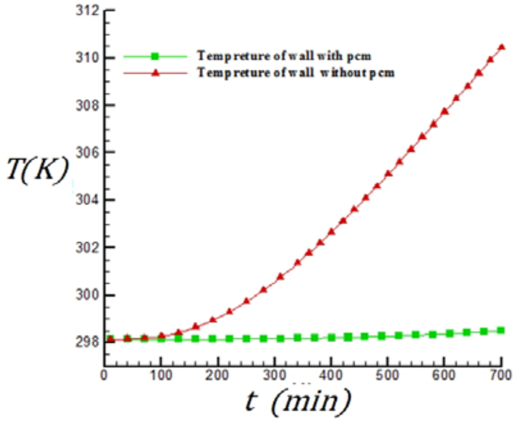

Figure 12: average interior wall surface temperature relative to time

Figure 13, shows the temperature contours of the wall with PCM and without PCM.

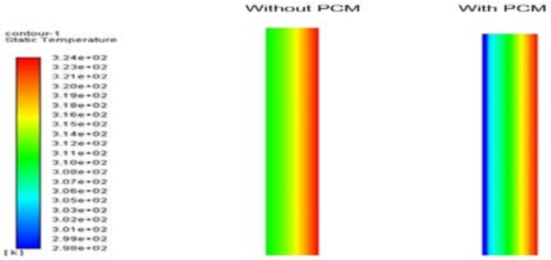

Figure 13: Temperature contours of the wall with PCM and without PCM.

The effect of adding nanoparticles with different concentrations on energy storage

One of the investigated parameters in this study is the effect of the type and concentration of the added nanoparticles. Figures. 14 and 15 show the effect of adding Cu nanoparticles with a concentration of 1% in the phase change material and nanoparticles of AL2O3 with similar concentrations and a phase change material without the presence of nanoparticles. According to these figures, the presence of Cu nanoparticles was more effective in increasing the proportion of volume fraction of the liquid and absorption of the thermal energy of the octadecane in a 12-hour interval. In Figures. 16 and 17, it can be seen that the addition of nanoparticles Cu and AL2O3 with a concentration of 3% produces a similar result, and in this case also adding nanoparticles Cu to the phase change material, has a better effect on the storage of thermal energy

As expected, the energy stored in the phase change material by adding nanoparticles Cu and AL2O3 at concentrations of 1% and 3% compared to the energy stored in PCM without nanoparticles, increases, and in both cases, the effect of improving energy storage by adding nanoparticles Cu was higher than that of AL2O3 nanoparticles. One of the reasons for this, is the higher thermal conductivity of copper than aluminum oxide. Therefore, in this study, since the effect of adding Cu nanoparticles in both concentrations of 1% and 3% was better than nanoarticles of AL2O3, the effect of Cu nanoparticles, in other concentrations is investigated.

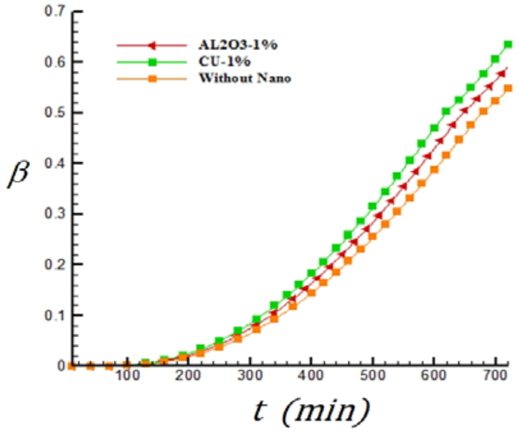

Figure 14: Liquid volume fraction changes relative to time for different nanoparticles at 1% concentration

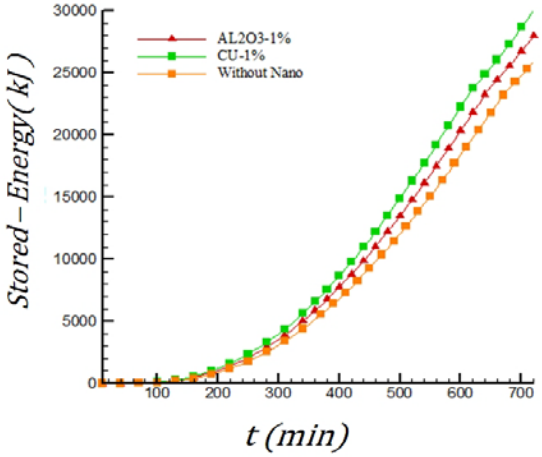

Figure 15: Changes in stored energy relative to time for different nanoparticles at a concentration of 1%

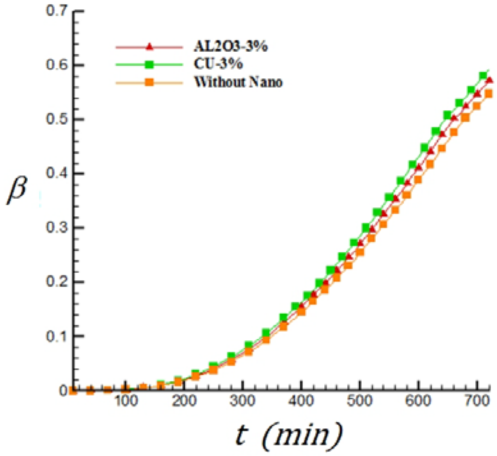

Figure 16: Liquid volume fraction change over time for different nanoparticles at a concentration of 3%

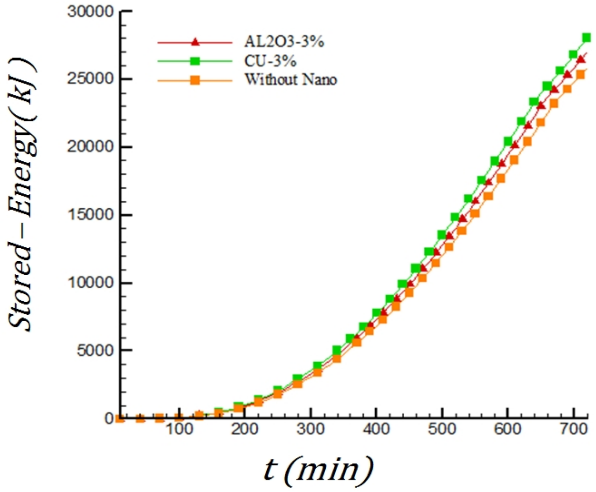

Figure 17: Changes in stored energy relative to time for different nanoparticles at a concentration of 3%

In Figures. 18 and 19, the effect of adding a nanoparticle Cu to the octadecane phase change material in a 12-hour time interval are shown in four concentrations of 0.5%, 1%, 3%, and 5%.

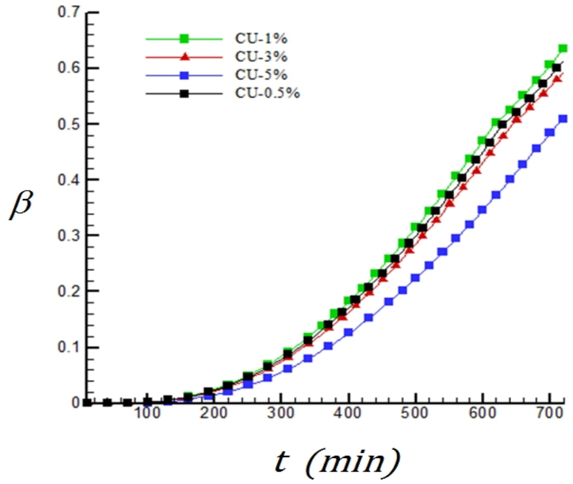

Figure 18: Changes in the volume fraction of liquid relative to time for copper nanoparticles at different concentrations

As can be seen, by adding a nanoparticle of copper to phase change material, the amount of the liquid volume fraction of the melted phase change material is increased, but for concenteration more than 1%, this parameter is reduced. The higher concentration of nanoparticles causes the higher density and therefore the thermal diffusion coefficient decreases and hence the heat transfer rate decreases and the melting time increases.

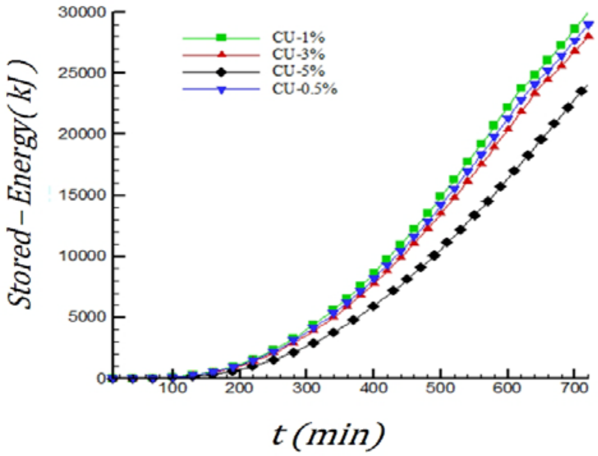

Figure 19: Changes in stored energy relative to time for different concentration of Cu nanoparticles

The effect of the phase change material layer position on its performance improvement

In this section, the effect of changing the position of the phase change material layer in the wall on its thermal performance has been investigated. A copper nanoparticle with a concentration of 1% was added to the phase change material of the octadecane with a thickness of 2 cm and the effect of the displacement of this layer in the wall was investigated. Figures. 20 and 21, show the change of the volume fraction of the liquid and stored energy over time in a 12-hour interval respectively. The PCM layer containing a 1% copper nanoparticle is placed between the plaster-soil and plaster layer.

Figures. 22 and 23, show the change of the volume fraction of the liquid and stored energy over time in a 12-hour interval respectively. The PCM layer contains a 1% copper nanoparticle is placed between the plaster-soil layer and brick. This mode is closer to the outer layer of the wall than to the previous one, and actually to the thermal energy source. Comparison of the graphs show that when the phase change material layer approaches the outer surface of the wall, it melts more rapidly than it does to the inner layer and actually stores more heat energy. In other words, when the layer of phase change material approaches the thermal energy source, energy passes through the layers of the wall.

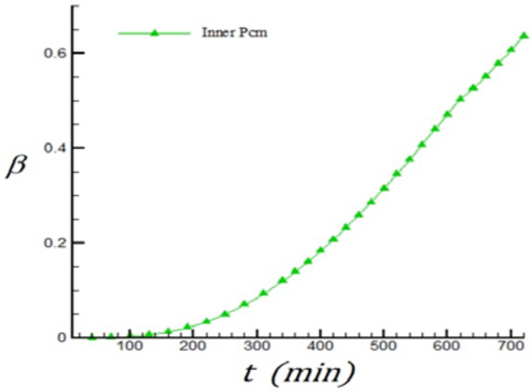

Figure 20: Changes in the volume fraction of the liquid relative to time in the octadecane containing 1% copper nanoparticles in the layer between the plaster-soil and plaster

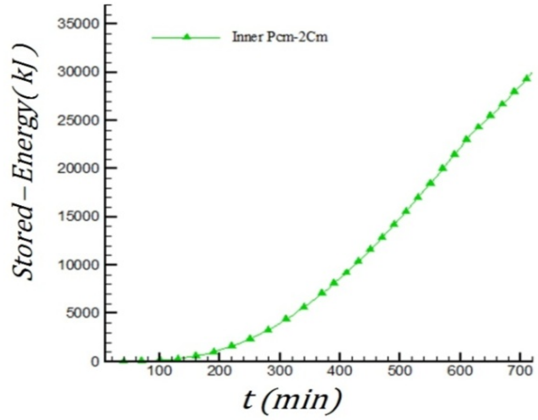

Figure 21: Energy savings relative to time in octadecane containing 1% copper nanoparticles in the layer between the plaster-soil and plaster

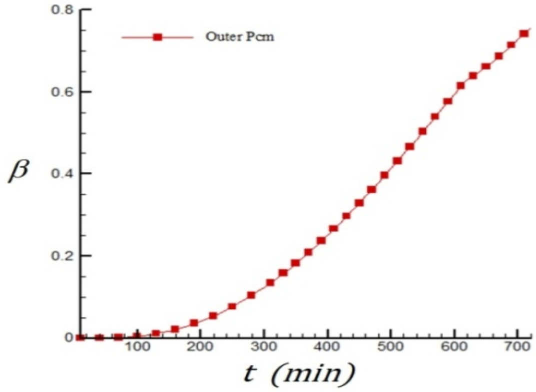

Figure 22: Changes in the volume fraction of the liquid relative to the time in the octadecane containing 1% copper nanoparticles in the layer between the plaster- soil and brick

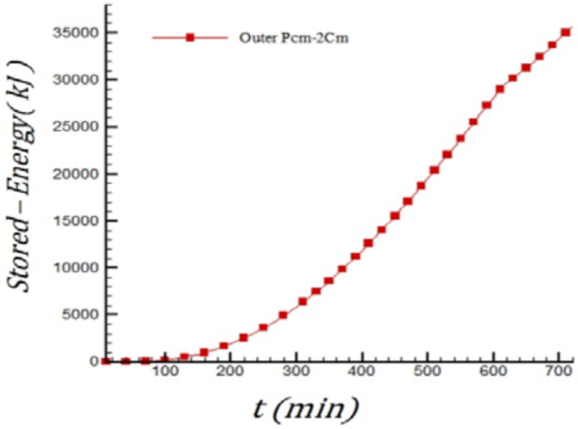

Figure 23: Energy savings relative to time in octadecane containing 1% copper nanoparticles in the layer between the plaster-soil and brick

Effect of thickness of phase change material on its performance improvement

In this section, the effect of the thickness of the phase change material in two positions of this layer inside the wall, as expressed in Section 3-4, is investigated. The octadecane phase change material contains copper nanoparticles with a concentration of 1%. Figure. 24, shows the change of the volume fraction of the liquid relative to the time in a 12-hour interval, when the PCM layer contains 1% copper nanoparticles in various thicknesses of 1, 1.1, 1.2, 1.5 and 2 cm, between the plaster-soil and the plaster layer.

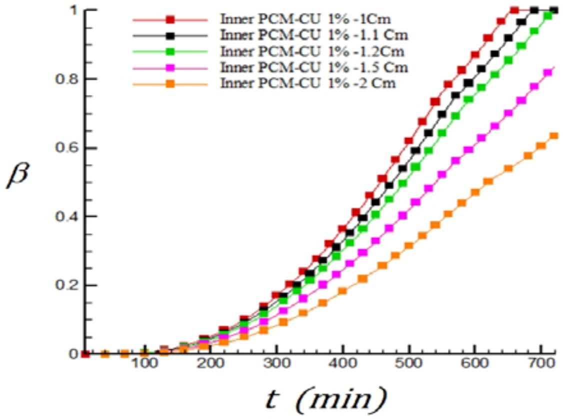

Figure 24: Liquid volume fraction changes relative to time in octadecane containing 1% copper nanoparticles with different thicknesses in the layer between plaster-soil and plaster

It is clear from the figure, the phase change material, in thicknesses of 1 and 1.1 cm, is not suitable due to the reaches of the volume fraction of the liquid to its maximum value at an earlier time than the 12-hour period, and a part of the thermal energy will not be absorbed due to the complete melting of this material before the full cycle of time. Also, in thicknesses of 1.5 and 2 cm, because of not completely melting the phase change material, it is not possible to use its full capacity, and only the weight and thicknesses of the wall are increased. Therefore these two thicknesses are not considered as optimal thicknesses. In the thickness of 1.2 cm, the amount of liquid fraction of the phase change material at the end points of the 12-hour cycle reaches its maximum. In other words, sufficiently close to 1, and therefore the maximum PCM capacity is used in this thickness. This thickness is therefore optimal thickness. Figure. 25, shows the stored energy changes over time in a 12-hour interval, when the PCM layer containing 1% copper nanoparticles has an optimum thickness of 1.2 cm and is placed between the plaster-soil and the plaster layer.

Figure. 26, shows the change of the volume fraction of the liquid relative to the time in a 12-hour interval, when the PCM layer contains 1% copper nanoparticles in the thicknesses of 1.5 and 2 cm, between the plaster-soil layer and brick. As it is clearly shown, at a thickness of 1.5 cm, the amount of liquid fraction of the phase change material at the end points of the 12-hour cycle, almost the maximum, thus the maximum capacity of PCM is used in this thickness and smaller thicknesses due to the melting of the total phase change material in the interval of up to 12 hours, as well as the impossibility of energy storage over the time, can not be optimum thickness. So the optimum thickness is 1.5 cm. In the thickness of 2 cm, due to the fact that the phase change material does not completely melted, it is not possible to use the total material capacity, and only the weight of the wall and thickness increases .

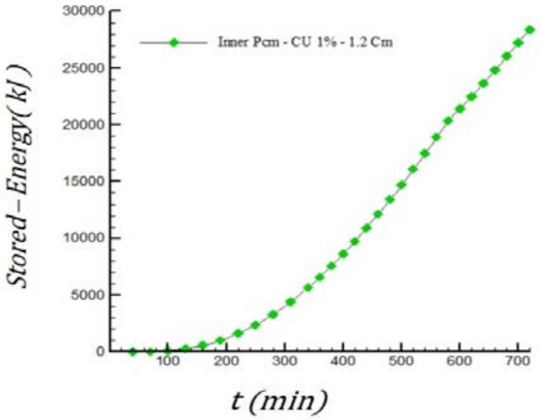

Figure 25: Changes in stored energy relative to time in octadecane containing 1% copper nanoparticles in an optimum thickness of 1.2 cm in the layer between plaster –soil and plaster

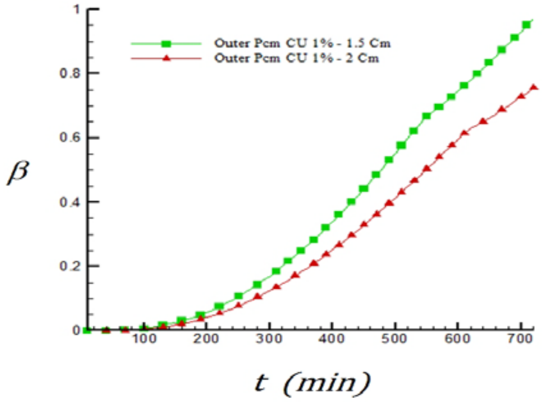

Figure 26: Changes in the volume fraction of the liquid relative to the time in octadecane containing 1% copper nanoparticles with different thicknesses in the layer between plaster-soil and brick

Figure. 27, shows the changes in stored energy over time in a 12-hour interval, when the PCM layer containing 1% copper nanoparticles has an optimum thickness of 1.5 cm and is placed between the plaster- soil layer and brick.

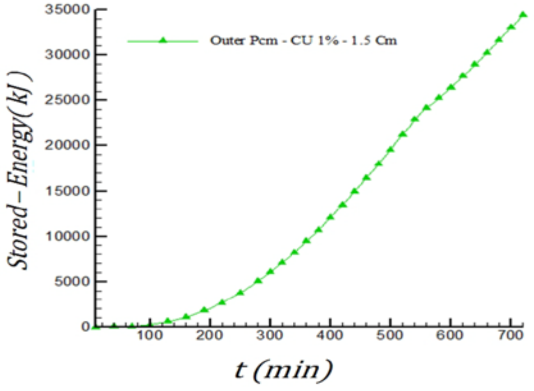

Figure 27: Stored energy relative to time in octadecane containing 1% copper nanoparticles in an optimum thickness of 1.5 cm in the layer between plaster-soil and brick

CONCLUSION

A review of the research shows that the comparison of the use of AL2O3 and Cu nanoparticles in the phase change material of the octadecane has not been done yet to improve energy storage in the building walls. Therefore in this research, numerical modeling and parametric analysis of the thermal performance of the phase change material layer by adding these nanoparticles were investigated. The results of this research can be summarized as follows:

- By adding the phase change material to the wall, the wall surface temperature has reached to 25.5 °C after 12 hours which without phase change material in the same state is 38 °C, and as a result, the presence of the phase change material has reduced the wall surface temperature by 13.5 ° C.
- The addition of Cu nanoparticles at a concentration of 1% to the octadecane and compare it with other concentrations of 0.5%, 3% and 5%, as well as adding the AL2O3 nanoparticles in different concentrations of 1% and 3% indicate that the copper nanoparticles with a concentration of 1% have better results in energy storage. However, no appreciable change in the internal temperature of the wall was observed in the presence of nanoparticles along with the octadecane phase change material.
- The addition of Cu nanoparticles of 1% to the phase change material of the octadecane causes energy storage to be 30.019 kJ, which in the case of phase change material without nanoparticles Cu or AL2O3, was 25.865 kJ (in 12 hours).
- Changing the position of the phase change material layer between the plaster-soil and plaster (the layer near the inner wall) to the position of the layer between the plaster-soil and the brick (layer near the outer wall) with 1% nano-particles of copper and 2 cm thickness, increased the energy storage from 30.019 kJ to 35.719 kJ.
- The optimum Thickness for a state where the phase change material containing 1% copper nanoparticles is located between the plaster-soil and plaster is 1.2 cm and between the plaster- soil and brick is 1.5 cm. This reduces the weight of the material consumed by 30% and reduces costs.

Nomenclature

Flow velocity	u_i
Pressure	P
Acceleration of gravity	g_i
Momentum source	S_i
Constant Coefficient	C
Enthalpy	H
Latent heat	ΔH
Sensible enthalpy	h
Specific heat capacity	C_p
Temprature	T
Latent heat of liquid	L
Conduction heat coefficient	k
Dispersion coefficient of the soluble matter	K_i
Mass fraction of the soluble matter	Y_i

liquidification gradient of the i-th component	m_i
Greek	
Density	ρ
Dynamical viscosity	μ
Volume fraction of liquid	β
Constant number	ε
Thermal expansion coefficient	α
Volume fraction of nanoparticles	φ
Subscripts	
Reference	ref
Base value	0
Nanofluid	nf
Solid	s
Liquid	f
Phase change material	pcm

References

Al-Abidi, AA, Mat, S., Sopian, K., Sulaiman, MY, & Mohammad, AT (2013). Internal and external heat transfer enhancement technique for latent heat thermal energy storage in triplex tube heat exchangers. *Applied thermal engineering* ,

Arıcı, M., Tütüncü, E., Kan, M., & Karabay, H. (2017). Melting of nanoparticle-enhanced paraffin wax in a rectangular enclosure with partially active walls. *International Journal of Heat and Mass Transfer*, *104*, 7-17.

Benli, H., & Durmuş, A. (2009). Performance analysis of a latent heat storage system with phase change material for new designed solar collectors in greenhouse heating. *Solar Energy*, *83*(12), 2109-2119.

Darzi, A. R., Moosania, S. M., Tan, F. L., & Farhadi, M. (2013). Numerical investigation of free-cooling system using plate type PCM storage. *International Communications in Heat and Mass Transfer*, *48*, 155-163.

Elgafy, A., & Lafdi, K. (2005). Effect of carbon nanofiber additives on thermal behavior or phase change materials. *Carbon*.

Gopalan, K. S., & Eswaran, V. (2016). Numerical investigation of thermal performance of PCM based heat sink using structured porous media as thermal conductivity enhancers. *International Journal of Thermal Sciences*, *104*, 266-280.

Jourabian, M., Farhadi, M., & Sedighi, K. (2014). On the expedited melting of phase change material (PCM) through dispersion of nanoparticles in the thermal storage unit. *Computers & Mathematics with Applications*, *67*(7), 1358-1372.

Leland, J., & Recktenwald, G. (2003, March). Optimization of a phase change heat sink for extreme environments. In *Ninteenth Annual IEEE Semiconductor Thermal Measurement and Management Symposium, 2003.* (pp. 351-356). IEEE.

Liu, C., Rao, Z., Zhao, J., Huo, Y., & Li, Y. (2015). Review on nanoencapsulated phase change materials: preparation, characterization and heat transfer enhancement. *Nano Energy*, *13*, 814-826.

Motahar, S., Alemrajabi, A. A., & Khodabandeh, R. (2017). Experimental study on solidification process of a phase change material containing TiO2 nanoparticles for thermal energy storage. *Energy conversion and management*, *138*, 162-170.

Nayak, K. C., Saha, S. K., Srinivasan, K., & Dutta, P. (2006). A numerical model for heat sinks with phase change materials and thermal conductivity enhancers. *International Journal of Heat and Mass Transfer*, *49*(11-12), 1833-1844.

Pakrouh, R., Hosseini, M. J., Ranjbar, A. A., & Bahrampoury, R. (2015). A numerical method for PCM-based pin fin heat sinks optimization. *Energy Conversion and Management*, *103*, 542-552.

Parameshwaran, R., Jayavel, R., & Kalaiselvam, S. (2013). Study on thermal properties of organic ester phase-change material embedded with silver nanoparticles. *Journal of thermal analysis and calorimetry*, *114*(2), 845-858.

Park, S., Lee, Y., Kim, YS, Lee, HM, Kim, JH, Cheong, IW, & Koh, WG (2014). Magnetic nanoparticle-embedded PCM nanocapsules based on paraffin core and polyurea shell. *Colloids and Surfaces A: Physicochemical and Engineering Aspects* ,

Raja, S., Prakash, S., Gokulnath, R., Krishnamoorthy, A., & Lillymercy, J. (2018). Pcm Based Thermal Energy Storage System Integrated with Solar Parabolic Trough Collector. *Journal of Engineering Science and Technology*, *13*, 40-51.

Sanusi, O., Fleischer, A., & Weinstein, R. (2010, June). An investigation into the solidification of nano-enhanced phase change material for transient thermal management of electronics. In *2010 12th IEEE Intersociety Conference on Thermal and Thermomechanical Phenomena in Electronic Systems* (pp. 1-6). IEEE.

Stritih, U. (2004). An experimental study of enhanced heat transfer in rectangular PCM thermal storage. *International Journal of Heat and Mass Transfer*, *47*(12-13), 2841-2847.

Zheng, N., & Wirtz, R. A. (2004). A hybrid thermal energy storage device, part 1: design methodology. *Journal of Electronic Packaging*, *126*(1), 1-7.

Zheng, N., & Wirtz, RA (2000). Methodology for designing a hybrid thermal energy storage heat sink. *ASME-PUBLICATIONS-HTD*,

Zheng, N., & Wirtz, RA (2001). Figures of merit for hybrid thermal energy storage units. *Proc., NHTC2001.*